

Sevenfold improvement of axial resolution in 3D widefield microscopy using two objective lenses

Mats G. L. Gustafsson, David A. Agard and John W. Sedat

*Department of Biochemistry and Biophysics
University of California, San Francisco
San Francisco, California 94143-0554*

ABSTRACT

A weakness of standard 3D microscopies – both confocal and widefield+deconvolution – is that their resolution is substantially worse in the axial direction than in the lateral plane. We describe two new widefield techniques with substantially improved axial resolution that actually exceeds the lateral resolution.

As is well known, the resolution is related to the angle over which the objective lens collects light. In our first technique, light is collected over an enlarged set of angles by using *two* objective lenses on opposite sides of the sample. The two image beams are combined coherently on the same CCD camera. Interference between the beams yields new, previously inaccessible sample information.

The second technique applies a similar concept to the illumination light in fluorescence microscopy. Light from an extended, spatially incoherent light source – such as a standard arc lamp – is split and directed through the two opposing objective lenses so as to create a narrow interference fringe at the focal plane in the sample. This spatial structure in the excitation light yields access to new sample information.

The two techniques can easily be used together; the combined technique promises an axial resolution improvement of a factor of seven over standard widefield microscopy.

Keywords: microscopy, optical microscopy, widefield microscopy, deconvolution, resolution, OTF, interference

1. INTRODUCTION

The first two sections of this paper discuss properties of existing modes of microscopy in order to create a framework in which to understand our new techniques.

1.1 Deconvolution widefield microscopy

Presently there are two main approaches to three-dimensional optical microscopy: computational deconvolution widefield¹ (also called optical sectioning), and scanning confocal microscopy². Our new techniques are variations on the former.

In deconvolution widefield microscopy, one uses a CCD camera to acquire a series of widefield images of the sample, while stepping the focus plane successively through the sample between each image. Each image contains in-focus information from the parts of the sample which are in the focal plane, but also blurred, out-of-focus information from the other parts of the sample. By analyzing the entire data set on a computer with the help of a known – preferably measured – point spread function (PSF), one then reconstructs the 3D structure of the sample, part of the result of this process being to remove the out-of-focus information.

While confocal microscopy has caught considerably more publicity in recent years, due in part to the fact that such systems have been commercially available much longer, deconvolution widefield microscopy remains an attractive technique with advantages for many applications. The most obvious advantage is the higher acquisition speed made possible by the inherent parallelity: confocal microscopy is a scanning technique, where data voxels are acquired one at a time, whereas a deconvolution widefield microscope using a 1024 x 1024 pixel CCD camera can acquire more than a million voxels in parallel. The widefield microscope also detects light very efficiently, due to the absence of a pinhole and the extreme quantum efficiency of the CCD. The high light efficiency allows higher signal levels with less photobleaching of the sample, and contributes to the speed advantage. Simple, high intensity light sources such as arc lamps can be used, and the excitation wavelength window can be

chosen freely, without being constrained to available laser wavelengths. While the resolution of confocal microscopy is higher in theory, the difference in practice is smaller³ since confocal data sets are normally displayed unprocessed, without the benefit of deconvolution. (It is certainly possible to apply deconvolution algorithms to confocal data, but doing so is hampered by the typically very low signal levels of a confocal microscope when it is operated with a small pinhole, as is necessary in order to access the high resolution information.)

In the end, the most important practical distinction between confocal and deconvolution microscopy may be the choice between on the one hand rapid display of the final data, at which the confocal method is superior because little computation is needed, and on the other hand speedy acquisition and low sample bleaching, where widefield deconvolution microscopy excels. For many applications, such as time-sequence imaging of dynamic cellular processes, the latter concerns are of considerable importance.

1.2 Axial and lateral resolution

Standard computational deconvolution widefield microscopy, like standard confocal microscopy, suffers from substantially lower resolution in the depth ("Z") direction than in the image ("X-Y") plane. The reasons for this are fundamental geometry, stemming from the finite wavelength of light and the limited angle over which the objective lens can collect light. By using two objective lenses, our new imaging modes expand the set of angles from which the sample can be accessed, thereby greatly increasing the Z resolution. Two other microscopy approaches already exist that employ two opposing objective lenses: 4Pi confocal microscopy⁴ and standing wave fluorescence microscopy⁵. Our techniques differs from both of these in that they do not require laser light sources, and of course differs from 4Pi confocal in that they are widefield techniques.

While the new techniques can be applied to many different modes of microscopy, we shall for specificity describe them in the context of fluorescence microscopy.

2. TRANSFER FUNCTIONS AND SUPPORTS

The output of a linear, translation invariant imaging process, such as widefield optical microscopy, can be described as a convolution of the actual sample structure with a "point spread function," PSF, characteristic of the imaging system. In Fourier space, this convolution corresponds to a multiplication of the sample Fourier transform with that of the PSF, called the optical transfer function (OTF). Deconvolution, in its simplest form, consists of dividing by this OTF, so as to recover the sample information. The problem is that the relevant OTFs are zero outside of a finite region (their "support") of Fourier space, so that no sample information from the region outside of the support is present in the image data. Thus the most important resolution-determining property of an imaging system, in the context of deconvolution, is the extent of the support of its OTF. In the following sections, we will show how simple geometrical arguments can be used to derive the well known shape of the support of the OTF for standard widefield microscopy, and then use the same reasoning to determine the substantially larger OTF supports pertaining to our new imaging modes.

2.1. Information content of the light field.

Consider a quasi-monochromatic light field $E(\mathbf{r})$ in a region away from the sources [Fig. 1 (a)]. Now take the Fourier transform of this field amplitude, i.e. separate it into its plane wave components. By the definition of "quasi-monochromatic," all these plane waves would have the same wavelength λ , though different directions. This means that their corresponding wave vectors \mathbf{k} all have the same length $|\mathbf{k}|=1/\lambda$ (or $2\pi/\lambda$, depending on convention), i.e. the Fourier transform $\mathcal{E}(\mathbf{k})$ of the field amplitude is nonzero only on a thin spherical shell of radius $1/\lambda$ around the origin of Fourier space [Fig. 1 (b)].

Since all we are considering so far is the field itself, and the laws of electromagnetism are linear and translation invariant, we conclude that the field amplitude $E(\mathbf{r})$ can be described as a convolution of the source emission amplitude distribution $A(\mathbf{r})$ with a "PSF" $P(\mathbf{r})$, namely the field amplitude from a point source at the origin. The Fourier space amplitude $\mathcal{E}(\mathbf{k})$ is then given by the product $\mathcal{A}(\mathbf{k})\mathcal{P}(\mathbf{k})$. We know from above that $\mathcal{E}(\mathbf{k})$ is nonzero only on the spherical shell of radius $1/\lambda$, so the same has to be true of $\mathcal{P}(\mathbf{k})$ [since there are no restrictions on $\mathcal{A}(\mathbf{k})$]. By spherical symmetry, the only possibility for $\mathcal{P}(\mathbf{k})$ is to have a uniform value on the shell, and be zero everywhere else – a more formal calculation confirms this. We thus know what sample information is carried by the light field: on the spherical shell of radius $1/\lambda$, the spatial frequency components of the field are simply proportional to those of the sample emission amplitude, while no off-shell sample information whatsoever is contained. As we shall see, the situation is actually somewhat better than this because we are dealing with incoherent sources.

Since all optical detectors measure the intensity, not the amplitude, of the light, and the fluorescent samples we are considering are incoherent sources and thus additive in intensity, we are more interested in the intensity of the field than in its instantaneous amplitude. The (time-average) field intensity is linear in the source intensities, and translation invariance still holds. Thus one can apply an argument entirely analogous to the one described above, and conclude that the *intensity* $I(\mathbf{r})$ of the field is a convolution of the sample emission *intensity* distribution $S(\mathbf{r})$ with the field *intensity* $Q(\mathbf{r})$ from a point source, so the corresponding Fourier space quantities are related by a product: $I(\mathbf{k}) = S(\mathbf{k})Q(\mathbf{k})$. Thus the quantity $Q(\mathbf{k})$, the Fourier transform of the field intensity from a point source, acts as an OTF from the sample to the light field.

The shape of $Q(\mathbf{k})$ can be found from the amplitude OTF $\mathcal{A}(\mathbf{k})$. The field intensity at the point \mathbf{r} of real space is the squared magnitude of the amplitude: $Q(\mathbf{r}) = |P(\mathbf{r})|^2 = P(\mathbf{r})P^*(\mathbf{r})$. In Fourier space this multiplication turns into a convolution: $Q(\mathbf{k}) = \mathcal{A}(\mathbf{k}) \otimes \mathcal{A}^*(-\mathbf{k})$, i.e. $Q(\mathbf{k})$ is the autocorrelation function of $\mathcal{A}(\mathbf{k})$. Because of the nature of an autocorrelation function, the support of $Q(\mathbf{k})$ is the set of difference vectors between points within the support of $\mathcal{A}(\mathbf{k})$. For the case under consideration, the unrestricted light field, the result of the convolution is thus a solid sphere of twice the radius of the shell [Fig. 1 (c)].

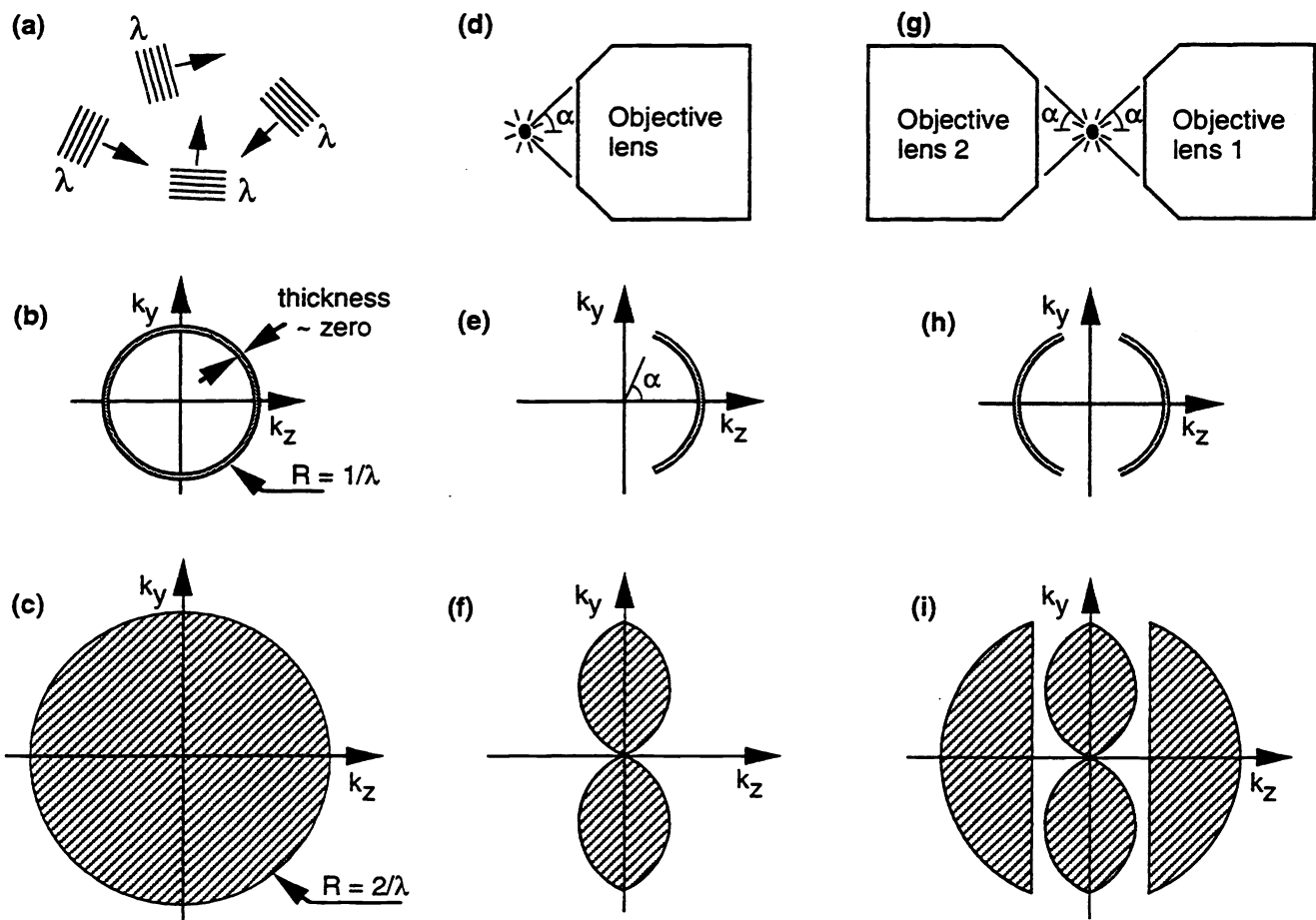


Figure 1. By definition, all Fourier components of a quasi-monochromatic light field have the same wavelength λ (a), i.e. they all reside on a spherical shell of radius $1/\lambda$ in Fourier space (b). This shell also describes the set of sample emission amplitude spatial frequencies about which any information is contained. The region from which *intensity* information is available (c) is the autocorrelation function of this shell, which has the shape of a solid sphere of twice the size. After a lens (d) with a finite acceptance angle α , only the amplitude information within a spherical cap (e) is left. The corresponding intensity information region (f), the autocorrelation function of this cap, is much smaller than (c), especially in the k_z direction. With two-lens detection (g), more amplitude information (h), and most of the available intensity information (i) can be accessed.

2.2 Accessible sample information in standard widefield microscopy.

In most optical systems, the sample can be observed only through a limited angle α [Fig. 1 (d)]. This simply has the effect of removing access to any components of the light amplitude (and thus the sample amplitude information) outside of the corresponding cone of Fourier space, leaving us with sample information only within a soup-bowl shaped region of Fourier space [Fig. 1 (e)]. Exactly as above, the region from which *intensity* information is accessible is the autocorrelation of this function, which (as is easy to convince oneself using the graphical procedure given above) has the support shown in Fig. 1(f). The region in Fig. 1(f) is thus the support of the OTF from the sample emission intensity to the field intensity. An actual optical system will contribute a second OTF, from the field to the recorded data, which has to be multiplied with $Q(\mathbf{k})$ to yield the total OTF of the system. However, all the fundamental limitations of optical imaging are determined by $Q(\mathbf{k})$, with no need to consider any other properties of the optical system than its aperture angle α . For the ideal systems normally considered in theory calculations, the second OTF is in fact unity, i.e. $Q(\mathbf{k})$ is the total OTF. Indeed, the region in Fig. 1(f) can be recognized as the support of the OTF for widefield microscopy described by many previous authors.⁶⁻⁸

3. DETECTING THROUGH TWO LENSES.

3.1 Accessible sample information

The essential feature of our first new technique is simply the presence of *two* objective lenses facing the sample from opposite sides [Fig. 1 (g)]. With the background of section 2 it is now easy to realize the advantage of such a system, and to determine its OTF support. A two-lens system collects light within two cones, each with opening angle α , thus its amplitude OTF, the region from which it can access sample amplitude information, consists of two bowl-shaped shells [Fig. 1 (h)]. As before, the intensity OTF is the autocorrelation function of this amplitude OTF. The same graphical procedure as above leads to the OTF support shown in Fig. 1 (i). (To arrive at the full extent of this region, the procedure has to be thought of in three dimensions – otherwise parts of the region that correspond exclusively to out-of-plane light rays may be overlooked.) Thus substantially more sample information can be accessed with a two-lens system.

3.2. Implementing a practical system

What is involved in creating a practical system to access this new sample information? The simplest idea, to use a separate camera for each lens, would not work – if it were attempted, each camera would in effect form a standard widefield microscope, and could access only the usual sample information described by the OTF in Fig. 1 (f). The new information is encoded in relative phase angles between the two image beams, which cannot be determined by studying each beam separately. However, if the two beams are combined coherently on a single detector, these relative phases cause detectable interference effects, so that this information can be accessed.

The most natural geometry for such a detector would be to combine the beams from opposite sides, just as they were collected [Fig. 2 (a)]. This would, however, require a transparent image detector of submicron thickness and flatness, which is not a practical device. Luckily, the alternative geometry in Fig. 2 (b) is almost entirely equivalent. In this geometry, where the two beams impinge on the detector from the same side, there are no unusual requirements on the detector. The total light efficiency of this setup is similar to that of standard widefield microscopy: there is a factor of two loss of light in the beam splitter, but twice as much light as normal is collected to start with because of the presence of the second objective lens.

The arrangement of mirrors has to be such that the two images have the same left-right parity on the detector, and are not rotated relative to each other. For a system where all beams are in one plane, this requirement is fulfilled simply

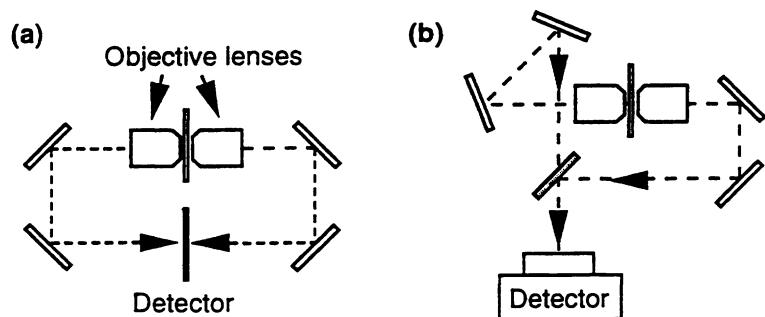


Figure 2. (a) A natural but impractical way to combine both image beams on a single detector. (b) An alternative, feasible arrangement.

by using an odd total number of reflections – thus the somewhat strange-looking arrangement in Fig. 2 (b). The second requirement for interference to take place is that the optical path lengths of the two beam paths from the focal plane to the beam splitter are equal to well within the coherence length of the emission light. This coherence length is determined by the bandwidth of the emitted light; for typical emission filter band widths of 20-50 nm, the coherence length is on the order of a few microns. Ideally, the relative phase of the two beams should be controlled to be zero to within a small fraction of 2π . This task can be performed by a path-length adjusting stage, or an electro-optical device. Thirdly, the focal planes of the two lenses must be made to coincide in the sample over the entire image, which can be done by adjusting the Z position and tilt of one objective lens, and the two images have to be superimposed in the lateral directions, which can be done by controlling the XY position of one objective lens and/or by tilt adjustments of various mirrors. Finally, the phase has to be made constant over the entire image (i.e. "phase tilt" and "phase curvature" have to be eliminated), which is also mainly a matter of alignment. If the two objective lenses are not well matched, it may also be necessary to adjust their relative magnification, which would require focusing elements inside the interferometric loop.

4. ILLUMINATING THROUGH TWO LENSES , AND THE COMBINED TECHNIQUE

Our second new technique, which applies most directly to fluorescence microscopy, uses a similar setup, but the essential point here is that both lenses are used for the illumination light. The light from a single, extended, spatially incoherent lightsource, such as a standard microscopy arc lamp, is divided by a beam splitter into two beams which are directed onto the sample through the two objective lenses [Fig. 3 (a)]. The sample fluorescence can then be viewed either through one [Fig. 3 (b)] or, with advantage, through both lenses [Fig. 3 (c)].

Consider the resulting illuminating light field at a point in combined focal plane in the sample. If the two illumination paths are completely symmetric, then purely by symmetry both beams will have the same amplitude and phase at this point, and thus interfere constructively. (Actually, if we take the vector nature of light into account, the electric field vector from each beam will in general have a small component along the Z axis. These axial components will cancel between the beams, while the larger lateral components interfere constructively.) Thus the illumination intensity at the focal plane would be not twice but four times that of each beam by itself. Now consider a point one quarter wavelength away from the focal plane. Since the two beam paths now differ in length by a half wavelength, we would expect any interference effects at this point to be destructive, i.e. we would expect the illumination intensity here to be no greater than twice that of a single beam. Thus there is a narrow plane, less than one half wavelength wide, of increased illumination intensity at the focal plane. (In fact, the intensity continues to oscillate in a damped fashion for a short distance on either side of the focal plane.) The apparent brightness of a fluorescent sample in this illumination field will thus oscillate as the sample is moved through focus. Note that this effect is a simple result of symmetry, and remains true regardless of the nature of the illumination upstream of the beam splitter; in particular it does matter whether the illumination is Köhler or critical, or any other arrangement. More importantly, it remains true even if the objective lenses are highly aberrated at the excitation wavelength, as long as the two lenses have the *same* aberrated behavior.

This spatial structure of the illumination field allows one to exceed the information limits described in section 3. To see how this can be the case, the important point to realize is that the limits on the "sample" information discussed there referred to the sample emission intensity $S(\mathbf{r})$, while what we really care about is the fluorophore density $\rho(\mathbf{r})$. These are related by $S(\mathbf{r}) = \rho(\mathbf{r}) L(\mathbf{r})$, where $L(\mathbf{r})$ is the local illumination intensity, which was tacitly assumed constant in section 3. In Fourier space, the corresponding relation is $S(\mathbf{k}) = \rho(\mathbf{k}) \otimes \mathcal{L}(\mathbf{k})$. If $L(\mathbf{r})$ is not constant, then $\mathcal{L}(\mathbf{k})$ has components away from the origin, and the convolution will mix information from different parts

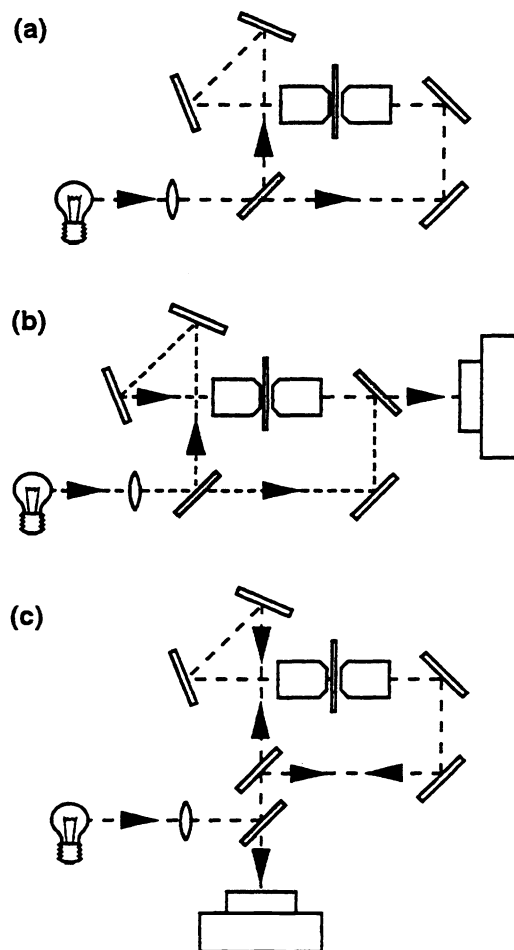


Figure 3. (a) Illuminating the sample through both lenses from a single incoherent light source. The sample emission can be viewed through one (b) or both (c) lenses.

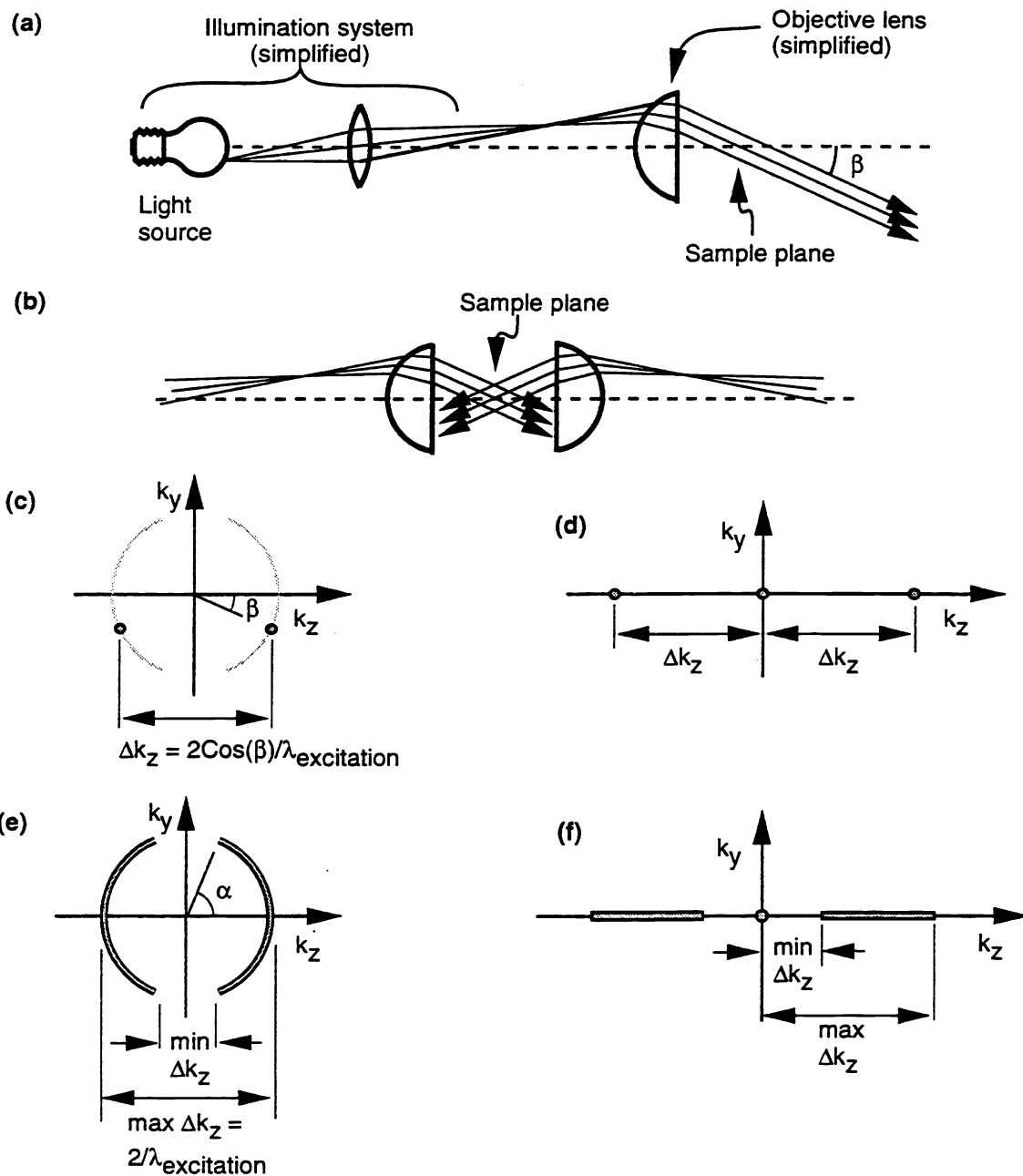


Figure 4. (a) In a typical microscope using Köhler illumination, any one point of the light source gets imaged into a beam of parallel rays in sample space. (b) In our new illumination method, each point of the light source is turned into two beams in sample space. (c) In Fourier space, this corresponds to two points (on the sphere of radius $1/\lambda_{\text{excitation}}$). The autocorrelation function of this, which describes the light intensity, consists of three points (d). The total light intensity in the sample is the sum of the contributions from all the points of the light source. The point pairs [as in (c)] from the various source points span the same double spherical cap as was shown in Fig. 2 (h), and the corresponding intensities [point triplets as in (d)] trace out the region shown in (f): two line segments plus a point at the origin. This is thus the region of support in Fourier space of the illumination intensity.

of $\rho(\mathbf{k})$. In particular, a point of $\mathcal{S}(\mathbf{k})$ within the accessible region of Fourier space (the OTF support) will receive information from different points of $\rho(\mathbf{k})$, some of which lie outside of the OTF support. Thus previously inaccessible sample information is brought within reach of our detectors. This is the basis for the resolution extension of our two-lens illumination technique (and also of confocal and standing wave microscopy).

It would seem from the previous paragraph that the information, while formally accessible, has been mixed together so as to be difficult to separate back out. Luckily this is not the case, provided that (a) the illumination structure is purely in the Z direction (i.e lateral translation invariance still applies) and (b) the structure is fixed in relation to the focal plane (as opposed to in relation to the sample) as one moves the sample through focus, so that Z translation invariance does apply to the image data set even though it does not apply to sample space at any given time. Under these conditions, the illumination structure behaves exactly as if it were a part of the point spread function – in fact, the system now has an effective point spread function that is the product of the illumination structure and the point spread function of the detection alone.

It follows that the effective system OTF is the convolution of the detection OTF with the Fourier transform $\mathcal{L}(\mathbf{k})$ of the illumination structure. Thus, we can easily construct the support of the effective OTF if we first determine $\mathcal{L}(\mathbf{k})$. To do so, let us assume for specificity that the illumination is Köhler, and consider first a single point \mathbf{p} of the light source. By the nature of Köhler illumination, each objective lens collimates this light into a parallel beam (a plane wave) in sample space [Fig. 4 (a), (b)]. The two beams intersect at some angle β which depends on the lateral position of the particular source point \mathbf{p} under consideration. The two beams are mutually coherent, since the light from any single source point is spatially coherent. In amplitude Fourier space, each of the plane waves corresponds to a single point on the spherical shell of radius $1/\lambda_{exc}$, i.e. the resulting amplitude structure $\mathcal{E}_{exc}(\mathbf{k}, \mathbf{p})$ is nonzero at only two points, separated by the distance $2\cos(\beta)/\lambda_{exc}$ [Fig. 4 (c)]. The corresponding intensity $\mathcal{I}_{exc}(\mathbf{k}, \mathbf{p})$, given by the autocorrelation of $\mathcal{E}_{exc}(\mathbf{k}, \mathbf{p})$, is nonzero at three points: the origin and two points on the k_z axis [Fig. 4 (d)] at a distance $2\cos(\beta)/\lambda_{exc}$ from the origin.

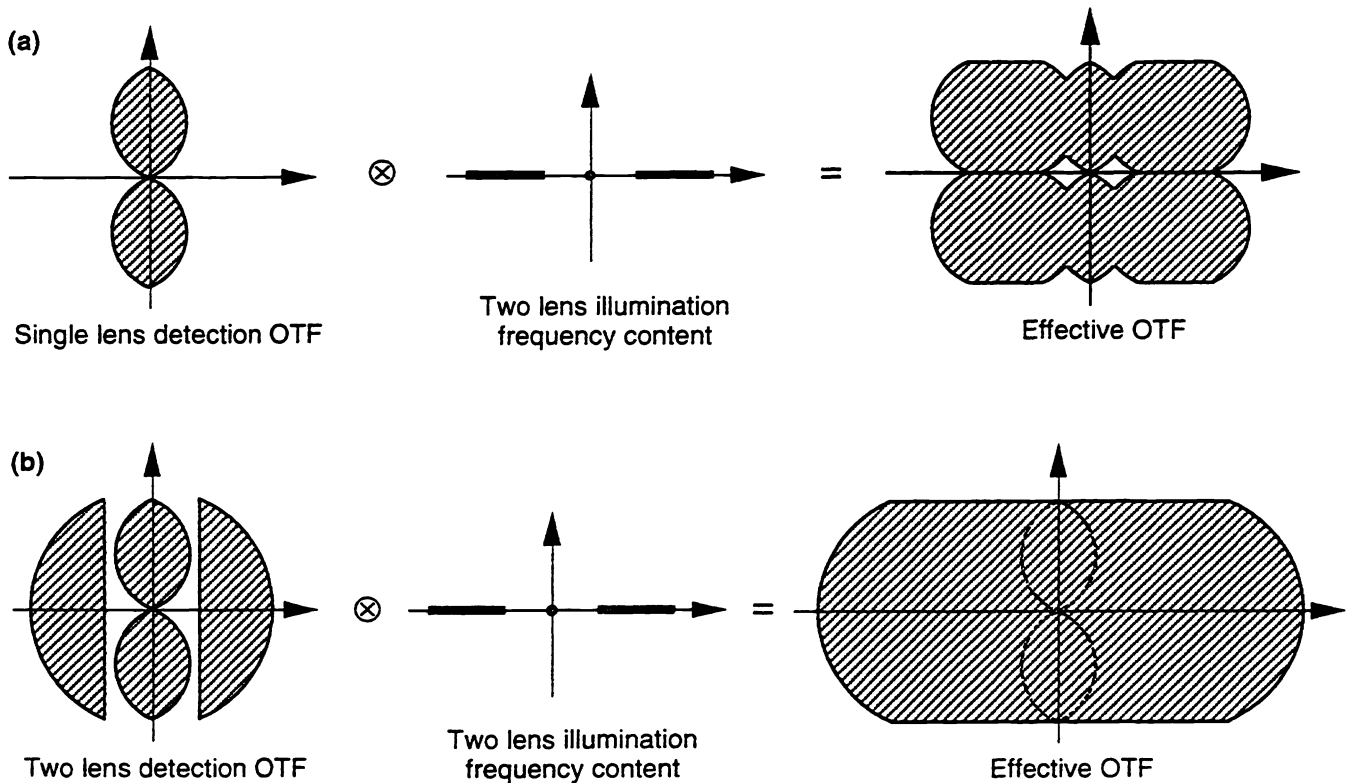


Figure 5. The OTF supports achieved by using the two-lens illumination method with (a) single and (b) dual lens detection. In (b), the OTF support for a standard widefield microscope is outlined for scale.

Since different source points are mutually incoherent, their intensity contributions add, both in real space and in Fourier space. Thus the total Fourier space illumination structure $\mathcal{L}(\mathbf{k})$ is the integral of $I_{\text{exc}}(\mathbf{k}, \mathbf{p})$ over all source points \mathbf{p} . The different source points will give rise to all values of the angle β between zero and the maximum angle α that the objective lenses can transmit [Fig. 4 (e)]. We conclude that the support of $\mathcal{L}(\mathbf{k})$ consists of two lines, from $\pm\text{Cos}(\alpha)$ to ± 1 , plus a point at the origin [Fig. 4 (f)].

As explained earlier, the system OTF is the convolution of $\mathcal{L}(\mathbf{k})$ with the appropriate detection OTF. One can use either the standard (one-lens) detection or, with advantage, our new two-lens detection mode. The resulting OTFs for these two cases are shown in Fig. 5 (a) and (b) respectively. The OTF for the combined technique extends to k_z values of $2/\lambda_{\text{emission}} + 2/\lambda_{\text{excitation}}$. As an example, consider the DNA-stain DAPI, excited at $\lambda_{\text{excitation}} = 360$ nm and detected at $\lambda_{\text{emission}} = 450$ nm, in a medium of refractive index 1.475 (glycerol) and viewed through lenses with an aperture angle α of 67.5° (as for NA=1.4 oil immersion lenses). The Z resolution (in the sense of the wavelength of the highest spatial frequency component that we can detect) for this case is 68 nm, an improvement of a factor of 7.3 compared with the Z resolution $\{[1 - \text{Cos}(\alpha)]/\lambda_{\text{emission}}\}^{-1} = 494$ nm of standard widefield microscopy for the same case. Assuming ideal deconvolution (but without taking into account the enhancement potential of external constraints such as positivity and spatial confinement), this corresponds, in a simple 1D model, to a full-width-at-half-max Z resolution of 41 nm.

The optimum alignment of the interferometric loop for the two-lens illumination scheme is identical to that for two-lens detection. Therefore, once the detection part of a system like that in Fig. 3 (c) has been aligned, the two-lens illumination is automatically pre-aligned when it is first turned on. The only possible caveat is due to the slightly different wavelengths of the excitation and emission light. This makes no difference as long as the two beam paths are perfectly symmetric. If, however, the two paths have strongly different amounts of second order dispersion (e.g. if one or both paths contain multilayer mirrors with complex phase characteristics), then the optimum value of the phase (the relative length of the two beam paths) will be subtly different for the illumination and emission light, and it could be beneficial to readjust the phase slightly to a compromise setting.

5. DISCUSSION

5.1. Comparison to other techniques

The concept of widefield microscopy detection through two objective lenses shares aspects with existing imaging technologies. Depending on viewpoint, it can be seen as the widefield equivalent of Type B 4Pi confocal microscopy,⁹ or as the application to microscopy of the interferometric image-superposition concepts of the emerging field of telescope-array optical astronomy¹⁰.

As is apparent from the discussion around Fig. 4, the new two-lens illumination scheme shares aspects of standing-wave microscopy, especially the excitation-field synthesis form of that technique.¹¹ In fact, from one viewpoint it is closely equivalent to standing-wave/excitation-field-synthesis illumination using scanning mirrors or an infinite number of mutually incoherent laser sources, but produces this effect with a single simple light source and no moving parts. Alternatively, the new illumination scheme can be thought of as similar to Type A 4Pi confocal microscopy, but achieving the Z-resolution enhancement effect of that technique at up to a million pixels in parallel.

The only existing optical microscopy technique that can achieve a Z resolution similar to that of our combined technique is "Type C" 4Pi confocal microscopy. When compared, the two techniques largely inherit the basic advantages and disadvantages of their respective parent techniques, confocal and widefield microscopy: 4pi confocal microscopy produces viewable data without the need to wait for computer processing, and does achieve higher lateral resolution when used with a small pinhole, but does so at the cost of much lower light efficiency and thus slower acquisition speed and more severe sample bleaching. As to the relative Z resolution of the two approaches, we see two arguments in favor of the new widefield technique: (a) unlike the case for the parent techniques, the 4Pi confocal technique has no advantage in terms of the amount of Z information it can access, while the widefield technique still has the advantage of easy computational enhancement due to its higher signal level, and (b) the new widefield method takes full advantage of the illumination effect even in wavelength regions where the objective lenses are not well corrected. In particular, this latter fact allows the method to be used to full effect with near ultraviolet excitation, which carries a resolution advantage due to the shorter wavelength, and in addition leaves more spectral room for multi-stain experiments and allows the use of important UV-excited nucleic acid probes such as DAPI. Finally, since it uses a simple incoherent light source, the new widefield technique affords full freedom to choose the excitation wavelength, without being restricted to available laser lines.

5.2. Limits of application

The same sample thickness limitation that affects 4Pi confocal and standing-wave microscopies apply to our new techniques as well: all these techniques are sensitive to phase errors caused by variations in the refractive index within the sample. For ideal operation, they require the sample to be "refractively thin," by which we mean that the *variation* of local optical thickness (i.e. of the integral dz of the sample refractive index) should be small compared to a wavelength. Thus, the more optically homogeneous a sample is, the thicker it can be without causing problems. What the actual thickness limit is for different types of samples will have to be determined by experience. Under *in-vivo* or near-*in-vivo* conditions, we believe that effective imaging will be possible on many biological systems at thicknesses of several microns, which would open up many aspects of cellular structure to investigation by high-resolution 3D optical imaging. Sample preparation protocols specifically aimed at optical homogeneity should be able to push these limits considerably further.

5.3. Future directions

We are presently constructing a prototype microscope with the ability to operate either with two-lens detection, with combined two-lens detection and two-lens illumination, or in the normal single-lens mode. Preliminary signs are quite encouraging, and we expect to be able to produce proofs-of-principle for both techniques in the near future.

Though we have so far described these new techniques in the context of fluorescence microscopy, they, and in particular the two-lens detection concept, can be applied to many other imaging modes as well. For example, two-lens detection used with one-sided bright field illumination turns into a combined transmission/ reflection bright field mode, with a weak-object OTF that consists of the central lobe and one of the side lobes of the OTF in Fig. 2 (i). Acquiring a second data stack with the reverse direction of illumination then supplies the other side lobe. Darkfield is even more similar to fluorescence, and supplies both side lobes (with the usual caveat that darkfield is a nonlinear imaging mode, so the normal OTF description does not apply in the strict sense).

6 SUMMARY

In summary, we have developed several new modes of 3D widefield optical microscopy, which promises axial resolution below 50 nm without compromising the high light efficiency and data acquisition rate of widefield microscopy.

7 ACKNOWLEDGEMENTS

This work was supported in part by funding from the Howard Hughes Medical Institute and through NIH grants number GM-25101 and GM-31627.

8. REFERENCES

1. Agard, D.A., Hiraoka, Y., Shaw, P. & Sedat, J.W., "Fluorescence Microscopy in Three Dimensions", *Methods in Cell Biology* Vol. 30 pp. 353-77, 1989.
2. Pawley, J.B., *Handbook of biological confocal microscopy*, Plenum Press, New York, 1990.
3. Carrington, W.A., Fogarty, K.E., Lifshitz, L. & Fay, F.S., "Three-dimensional Imaging on Confocal and Wide-field Microscopes", in *Handbook of Biological Confocal Microscopy*, ed. J.B. Pawley, pp. 141-61, Plenum, New York, 1989.
4. Hell, S. & Stelzer, E.H.K., "Properties of a 4Pi confocal fluorescence microscope", *Journal of the Optical Society of America A (Optics and Image Science)* Vol.9, no.12, pp. 2159-66, 1992.
5. Bailey, B., Farkas, D.L., Lansing Taylor, D. & Lanni, F., "Enhancement of axial resolution in fluorescence microscopy by standing-wave excitation", *Nature* Vol. 366, no.6450, pp. 44-8, 1993.
6. Streibl, N., "Three-dimensional imaging by a microscope", *Journal of the Optical Society of America A (Optics and Image Science)* Vol. 2, no.2, pp. 121-7, 1985.
7. Sheppard, C.J.R. & Mao, X.Q., "Three-dimensional imaging in a microscope", *Journal of the Optical Society of America A (Optics and Image Science)* Vol. 6, no.9, pp. 1260-9, 1989.

8. Beware, if comparing in detail, that many authors apply approximations such as paraxiality, and thus arrive at subtly different regions.
9. Hell, S.W., Stelzer, E.H.K., Lindek, S. & Cremer, C., "Confocal microscopy with an increased detection aperture: type-B 4Pi confocal microscopy", *Optics Letters* Vol. 19, no.3, pp. 222-4, 1994.
10. *Proceedings of the SPIE 2200: Amplitude and Intensity Spatial Interferometry II*, Kona, Hawaii, 1994 (entire volume).
11. Lanni, F., Bailey, B., Farkas, D.L. & Taylor, D.L., "Excitation field synthesis as a means for obtaining enhanced axial resolution in fluorescence microscopes", *Bioimaging* vol.1, no.4, pp. 187-96, 1993.